

The Fourth Italian Workshop on Landslides

Kinematic segmentation and velocity in earth flows: a consequence of complex basal-slip surfaces

Luigi Guerriero^{a*}, Paola Revellino^a, Lara Bertello^b, Gerardo Grelle^a, Matteo Berti^b,
Francesco Maria Guadagno^a

^aDepartment of Science and Technology, University of Sannio, Benevento, Italy

^bDepartment of Biological, Geologic and Environmental Sciences, University of Bologna, Bologna, Italy

Abstract

We investigated relations between geomorphic structures, movement velocity, and basal-slip surface geometry within individual kinematic domains of two large earth flows in the Apennine Mountains of southern Italy: the “Montaguto” earth flow and the “Mount Pizzuto” earth flow. Our analyses indicated that the earth flows are composed of distinct kinematic zones characterized by specific deformational patterns and longitudinal velocity profiles. Variations in velocity within individual kinematic zones is controlled by the geometry of the basal-slip surface, and, in particular by local variations in slope angle. Slip-surface geometry and slope also seem to control the density of extensional structures in driving earth-flow elements.

© 2016 The Authors. Published by Elsevier B.V. This is an open access article under the CC BY-NC-ND license (<http://creativecommons.org/licenses/by-nc-nd/4.0/>).

Peer-review under responsibility of the organizing committee of IWL 2015

Keywords: earth flow; velocity; basal-slip surface; structure; kinematic zone; GPS; southern Italy

1. Introduction

Periodic movement of large, thick landslides on irregular basal-slip surfaces modifies the topographic surface, creates deformational structures (i.e. faults and folds), and influences the location of hydrologic features like springs, ponds, and streams^{1,5,9}. Earth-flow movement often alternates between long periods of relatively slow movement and relatively rapid surges in movement²². Slow movement can persist for days, months, or years⁴. Surges in earth-flow movement are less common and earth flows capable of surging move in a slow persistent manner most of the time²².

* Corresponding author. Tel.: +39-333-9760824.

E-mail address: luigi.guerriero@unisannio.it

Velocities of earth flows during slow, persistent, movement range from less than 1 mm/d to several meters per day²². However, velocity of several meters per day have been observed also during earth flow surge¹⁴. The highest localized earth-flow surge speed documented in the literature is 0.13 m/s²¹.

Velocity profiles in earth flows generally reveal the existence of well-defined basal and lateral shear-surfaces normally associated with sliding movement in fine-grained soils^{20,22,7,3,12}. The geometry of the basal-slip surface, which can be controlled by geologic structures and ancient earth-flow deposits^{16,26} can control the position of deformational structures and spatial variations in the rate of displacement, both of which are responsible for kinematic segmentation of the landslide^{2,8,16}. Thus, large earth flows are often composed of several distinct kinematic zones^{2,16,17,19}. In earth flows with basal-slip surfaces with riser and tread geometries, individual kinematic zones can be characterized by stretching (extension; i.e. driving elements) at risers in the upper part of the zone and shortening (compression; i.e. resisting element) at treads in the lower part of the zone².

On the basis of this knowledge, we investigated the relation between structures, velocity distributions, and basal-slip surface geometry within individual kinematic domains of two large earth flows in the Apennine Mountains of southern Italy: the “Montaguto” earth flow and the “Mount Pizzuto” earth flow. Both earth flows are located on structurally complex slopes. At Montaguto, we used the mapped distribution of structures and hydrologic features¹⁶, the geometry of the basal-slip surface beneath individual domains¹⁶ and successive sets of orthorectified aerial-photos to determine the surface deformation and velocity distribution of 25 natural objects within the fastest moving kinematic zone near the longitudinal center of the earth flow (i.e., the “neck”kinematic zone). At Mount Pizzuto we used the mapped distribution of structures and hydrologic features¹⁹; 2 hand-excavated boreholes, 7 shallow-seismic profiles and 27 ambient seismic noise acquisitions (HVSr); and RTK-GPS surveys of a network of 35 benchmarks to define the geometry of the basal-slip surface and determine the distribution of average flow velocities.

Throughout this paper terminology and classifications from structural geology is used to describe deformational structures forming earth flow surface, because they accurately depict the geometry and relative sense of displacements for the structures that were observed¹⁴.

2. The Montaguto earth flow

2.1. Earth flow description

The Montaguto earth flow affects the southern slope of La Montagna Mountain in southern Italy. It is located along the southern side of the Cervaro River valley at UTM coordinates of approximately 4566000 N and 518000 E. The earth flow is approximately 3 km long and involves 4 to 6 Mm^{3,11,14}. Its width ranges from 75 m at the earth-flow neck to 450 m in the upper part of the earth-flow source area. The total elevation difference from the toe, adjacent to the Cervaro River, to the top of the 90 m high headscarp, is approximately 440 m. The average slope angle, excluding the headscarp, is approximately 7.2°.

Earth-flow displacement occurs mainly along basal and lateral faults and shear zones. Lateral strike-slip faults are better expressed in the lower part of the source area, where they are commonly associated with flank ridges, and along the earth-flow transport zone, where fault segments reached a length of few hundreds of meters⁸. Shear zones are distributed along earth-flow boundary between fault segments and locally between active lateral strike-slip faults and between active lateral strike-slip faults and the earth-flow margin. The earth-flow travel path has a sharp bend that is strongly influenced by inactive earth-flow deposits and geologic structures²⁶.

The earth-flow material is from the Miocene Flysch of the Faeto formation and the Pliocene Villamaina formation, both of which outcrop on the southern slope of La Montagna Mountain¹¹. The Flysch of the Faeto formation and the Villamaina formation are lithologically complex, containing a wide variety of clay beds, marls, sandstones, and conglomerates¹¹. This geological complexity influences groundwater flow and many springs are present from 600 m above sea level to the top of the La Montagna Mountain⁶. Several groups of springs are located along the western flank of the earth-flow and at/near the head of earth-flow (Fig. 1).

Historical information^{14,18} showed that the Montaguto earth flow has been periodically active during the last decades and the first activation dates back to 100 years ago. In particular, the 1958 and the 2006 reactivations were the largest in terms of mobilized volume and changes in earth-flow length and morphology¹⁵.

2.2. Deformational structures and segmentation

Guerriero et al.¹⁴ mapped deformational structures and hydrologic features of the Montaguto earth flow in May 2010. Structures were mapped using real-time kinematic (RTK) Global Positioning System (GPS) technique¹⁰, with a dual-frequency GPS receiver. Horizontal accuracy during field mapping ranged from 2 to 7 cm; 3D accuracy ranged from 3 to 11 cm. The mapped distribution of the structures was used to identify kinematic zones formed by major paired driving and resisting earth-flow elements².

Figure 1a shows the configuration of the Montaguto earth flow in 2010. Deformational structures within the flow include normal faults and tension cracks, indicating earth-flow stretching; thrust faults, back-tilted surfaces, flank ridges, fold structures, and pressure ridges, indicating earth-flow shortening; back-tilted surfaces indicating backward rotation; and strike-slip faults bounding the moving core of the flow. Five active kinematic zones containing structures indicating both stretching and shortening were recognized along the earth flow: the Head, the Hopper, the Neck, the Body and the Active Toe (Fig. 1a). Two kinematic zones were in the earth-flow source area. The upper zone, the Head, consisted of the headscarp, internal landslides, back-tilted surfaces with associated ponds and a cluster of thrust faults. The lower zone, the Hopper, consisted of (in upslope to downslope progression) a cluster of normal faults, flank ridges bound by strike-slip faults, and thrust faults. Downslope from the Hopper, the earth-flow Neck kinematic zone was delineated at its upslope end by a group of normal faults (shown as a single fault because of scale limitations) and at its downslope end by a thrust fault and a back-tilted surface. As the earth flow emerged from the Neck, it changed direction and moved to the southeast. The Body kinematic zone, downslope from the Neck, contained paired normal faults and thrust faults and discontinuous strike-slip faults that were associated with flank ridges at the downslope end of the zone. Downslope from the Body, the Active Toe zone was defined by normal faults at its upslope end and thrust faults at its downslope end. Strike-slip faults periodically formed at the advancing front of the Active Toe through 2010, as it continued to advance downslope and spread laterally. For further details regarding the evolution of structures and kinematic zones see Guerriero et al.¹⁶.

2.3. Basal-slip surface geometry

Guerriero et al.¹⁶ used data from boreholes, pit excavations, static cone penetration tests, seismic profiles, and difference DEMs to reconstruct the geometry of the basal-slip surface. In total, they used 26 data points to constrain the geometry of the basal-slip surface along the longitudinal profile of the flow: 1 point within the Head zone, 5 within the Hopper, 3 within the Neck, 6 within the Body, and 11 within the Active Toe (Fig. 2). The depth of the basal-slip surface ranged from 14 m within the Active Toe to about 4 m in the Neck (Fig. 2). Overall, the basal-slip surface (Fig. 2) is a repeating series of steeply sloping surfaces (risers) and gently sloping surfaces (treads). The upslope ends of each kinematic zone are at risers and the downslope ends are at treads. Normal faults occur at risers and thrust faults occur at treads. Within each kinematic zone, the overall shape of the slip surface is concave upward, whereas at the transition areas between zones, the shape is convex upward. In general, the thinnest parts of the earth flow are at risers and transition areas, and the thickest parts are at treads. Individual pairs of risers and treads formed quasi-discrete kinematic zones that operated in unison to transmit pulses of sediment along the length of the flow¹⁶ (Fig. 2).

3. The Mount Pizzuto earth flow

3.1. Earth flow description

The Mount Pizzuto earth flow¹⁹ is among the most active earth flows of the Benevento province^{13,27}. It affects the northeastern side of Mount Pizzuto from about 720 m above sea level (a.s.l.) to about 550 m (a.s.l.), and involves an estimated volume of 300,000 m³ of fine-grained flyschoid material. From a geological viewpoint, the Mount Pizzuto earth flow is located at an overthrust fault between i) the Argille Varicolori formation forming the upper part of the slope, where the flow source area is located, and ii) the Flysch of San Bartolomeo formation outcropping in the middle and lower parts of the slope²⁵. The tectonic contact between these formations materializes a WNW-ESE trending thrust fault that constitutes a weak zone where several landslide source-areas are located²⁵. The Mount

Pizzuto earth flow has been periodically active in the last decades and, as described by local people, early in 2006, it surged damming the Ginestra torrent at its toe. The earth-flow dam induced episodic floods that periodically damaged a segment of a local road and power and telephone service lines. In 2008, a man-made ditch was excavated along the torrent course and a large diameter drain was installed. These mitigation structures worked until early 2011, when a flood destroyed the drain and the local road and service lines. In October 2015, two new flooding events destroyed the local road and the service lines and enlarged dramatically the bed of the Ginestra torrent.

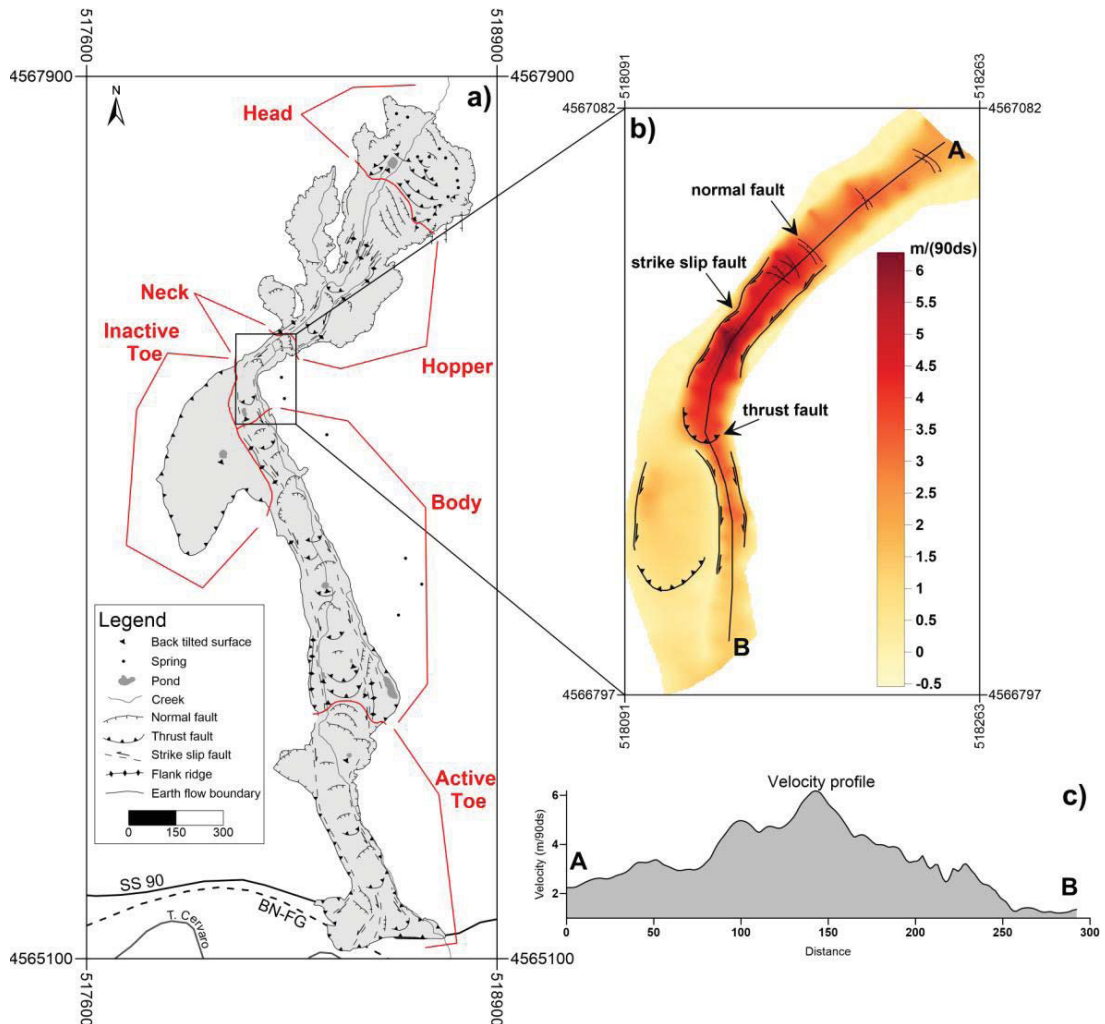


Fig. 1. Maps showing a) structures and kinematic zones of the Montaguto earth flow and b) structures and velocity within the earth flow Neck. C) Velocity profile of the earth flow Neck, see b) for velocity profile position.

3.2. Deformational structures and segmentation

Guerriero et al.¹⁹ mapped deformational structures and hydrologic features of the Mount Pizzuto earth flow in September 2014. Structures were identified, mapped, and processed in the same way as at the Montaguto earth flow. Also as at Montaguto, the mapped distribution of the structures was used to identify kinematic zones formed by

major paired driving and resisting earth-flow elements². The structures and zones shown in Figure 3 are simplified from the highly detailed map of Guerriero et al.¹⁹.

Five kinematic zones were recognized in the earth flow: a Head, Hopper, Neck, Body, and Toe. The Head of the earth flow (Fig. 3) consists of two coalescing branches, each containing extensional and compressional structures. The northern branch contains a group of normal faults delineating a natural amphitheater. Downslope from this first set of normal faults, the earth-flow core is bounded by discontinuous strike-slip faults and contains both normal faults, tension cracks, and thrust faults. Segments of strike-slip faults are arranged as left- or right-stepping en-echelon arrays and the stepping direction controls the width of the earth flow. Segment lengths range from 4 to 30 meters. The azimuths of tension-crack openings ranges from 30° counterclockwise to 30° clockwise from the direction of the strike-slip faults forming the left flank of the flow. The southern branch contains a group of normal faults forming the main headscarp (from 2 to 4 m high) and the structure distribution is similar to the northern branch. Thrust faults form back-tilted surfaces and ponds where the northern and southern branches join. Downslope from the Head, a highly fractured area marks the beginning of the Hopper (Fig. 3). This kinematic zone is laterally bound by inward-stepping segments of strike-slip faults that accommodate earth-flow narrowing. The earth-flow Hopper is divided into three major deformation zones: i) an upper zone characterized by normal faults and tension cracks, ii) a middle zone containing a group of normal faults that face downslope in its upper part and tend to face toward the flanks in the lower part, and iii) a lower zone characterized by thrust faults associated with back-tilted surfaces containing ponds. The Neck contains the narrowest section of the earth flow (i.e. the neck). Within the Neck, the moving core is bound on both flanks by discontinuous strike-slip faults that step inward at the upper end of the Neck and outward at the downslope end of the Neck. Also within the Neck is a highly fractured area that evolves downslope into a cluster of downslope-facing normal faults. The Neck ends at a cluster of thrust faults. Downslope from the Neck, the Body is bound by segments of strike-slip faults, locally alternating with en-echelon sets of tension cracks. The upper part of the Body is characterized by a group of extensional features (i.e. normal faults and tension cracks) and a thrust fault. Downslope, a pull-apart basin delineated by extensional and compressional structures is present at steps in strike-slip faults forming the right flank of the flow. Toward the longitudinal axis of the flow, longitudinal segments of thrust faults form the suture line between the material mobilized in April 2014, and the material leaving a structural basin. Thrust faults in this part of the earth flow mark the end of the Body kinematic zone. The earth flow Toe consists of a smaller, upper, extensional zone with a group of normal faults and a larger compressional zone with large thrust faults associated with back-tilted surfaces. Most of these back-tilted surfaces contain ponds.

3.3. Basal-slip surface geometry

We used 2 boreholes, 7 shallow-seismic profiles (i.e. ReMi-MASW) and 27 ambient seismic noise acquisitions (i.e. HVSR) to detect the depth of the basal slip-surface along the Mount Pizzuto earth flow¹⁹ (Fig. 4). The boreholes were hand-excavated using a helicoidal auger. Shallow seismic profiles were carried out using the Multichannel Analysis of Surface Waves (MASW) method; and Soilspy equipment (manufactured by Micromed). The acquisitions were completed using 8 vertical geophones (4.5 Hz) with 2 m spacing, in both passive (ReMi) and active (MASW) mode. The surveys were interpreted with Grilla (Micromed Software) with a manual procedure. The HVSR^{23,24} analysis was carried out with Tromino (manufactured by Micromed).

In total, we used 29 data points to constrain the basal-slip surface geometry along the longitudinal profile of the flow: 4 points within the Head zone, 6 within the Hopper, 4 within the Neck, 8 within the Body, and 6 within the Active Toe (Fig. 4). The positions of boreholes and ReMi-MASW is reported in figure 4a using red symbols. HVSR measurements were completed at monitoring points installed along the flow (Fig. 4). Monitoring point positions can be seen in figure 4a as blue symbols on the black line which indicates the earth-flow ground surface. The depth of the basal-slip surface ranged from 6 m within the Active Toe to about 2 m in the Neck (Fig. 4). Overall, the basal-slip surface (Fig. 4) is a repeating series of steeply sloping surfaces (risers) and gently sloping surfaces (treads). The upslope ends of each kinematic zone are at risers and the downslope ends are at treads. Risers and thread are better expressed in terms of longitudinal extension and change in slope angle in the Head, Hopper, and Neck.

4. Methods used to determine movement velocity

4.1. Measuring earth-flow displacement from successive sets of orthoimages at Montaguto

We measured the displacement of 25 natural and artificial objects (i.e., large rock fragments, drain pipes, etc.) on the surface of the Neck kinematic zone of the Montaguto earth flow, visible in successive sets of satellite orthoimages. The orthoimages were Eros-B digital orthorectified images taken on 25/05/2010 and 25/08/2010, respectively. The EROS-B satellite acquires panchromatic images with a nadiral Ground Sampling Distance (GSD; i.e., spatial resolution) of 0.7 m (single sided pixel dimension) and the radiometric resolution is within a spectral range of 0.5 to 0.9 μm . Objects consisting of groups of pixels were recognized on the basis of their geometry and color (i.e., Digital Number) distribution. Corners of object were visually picked from a computer display, and displacement was manually measured in a GIS. The irregularly distributed displacement values were interpolated to produce a displacement map. Interpolation was completed using the Inverse power to a distance method and deformational structures were used as breaklines. The error in displacement was assigned on the basis of the computed east-west and north-south root mean square errors in the position of 16 stable ground control points. In the Easting direction, the $2 \times \text{RMS}$ values ranged from 0.04 to 0.12 m, but averaged about 0.08 m. In the Northing direction, the $2 \times \text{RMS}$ values ranged from 0.02 to 0.18 m, but averaged about 0.06 m. Considering that Easting and Northing RMS values are not equal, the error in displacement depends on the azimuth of the displacement vector, with the Easting and Northing RMS values being the maximum and the minimum errors, respectively.

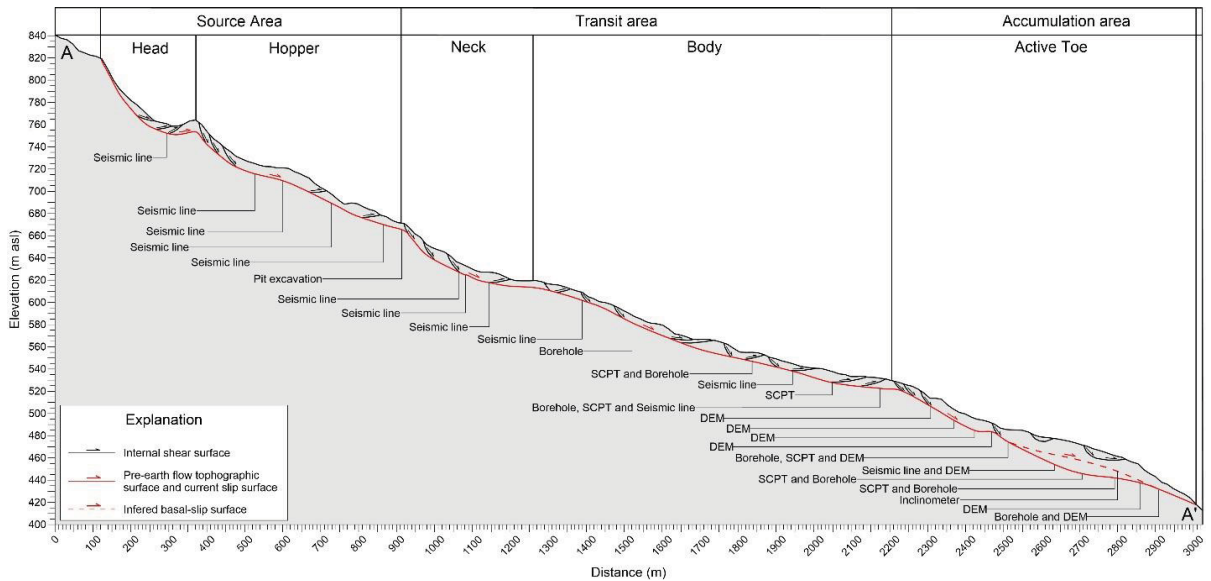


Fig. 2. Longitudinal profile of the Montaguto earth flow showing the geometry of the basal-slip surface. Types of data used to control the position of the basal-slip surface are shown (e.g., seismic line and pit excavation). SCPT is static cone penetration test.

4.2. Installation, distribution and monitoring of GPS points at Mount Pizzuto

In April 2014, we installed 35 monitoring points on the Mount Pizzuto earth flow. Monitoring points were placed on the earth flow along its approximate longitudinal axis. Exceptions were the monitoring points 9 to 19 that were installed off this axis within the Hopper and the upper part of the Neck (Fig. 3). Monitoring points were distributed along the earth flow on the basis of field mapping used to identify major kinematic zones. In each kinematic zone, we installed from 4 to 9 points. The points, placed with a clear view of the sky, were surveyed using Real Time Kinematic GPS technique using a Leica Viva-Net rover equipped with a Leica GS08 dual-frequency antenna. Real

time correction for high-accuracy measurement was obtained through the “Regione Campania”(Campania Region) network. The horizontal and vertical RMS errors in GPS positions, ranged from 1 to 3 cm, and 2 to 5 cm, respectively. All of the points were surveyed during 2, 1-day long GPS campaigns with a period of 395 days between campaigns. The first survey was in April 08, 2014. Earth-flow displacement and direction were determined from measured GPS positions imported into a GIS.

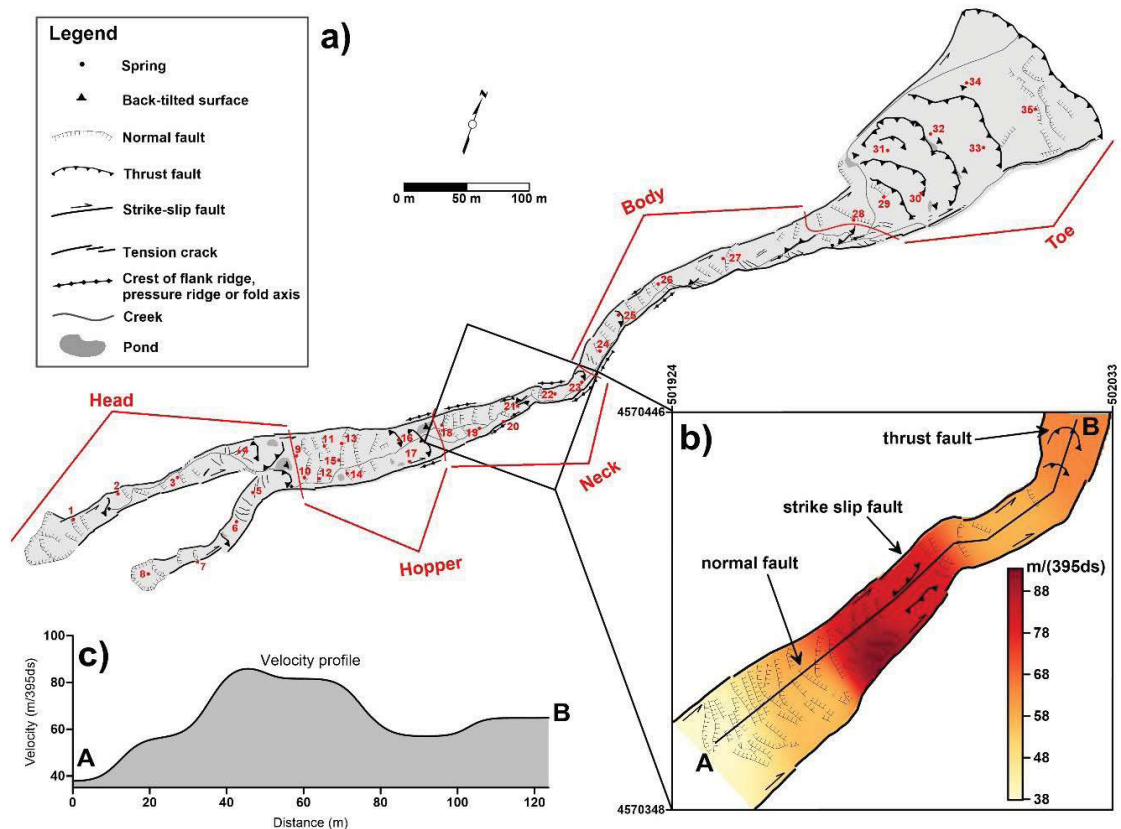


Fig. 3. Maps showing a) structures, kinematic zones, and monitoring points at the Mount Pizzuto earth flow, and b) structures and velocity within the earth flow Neck. c) Velocity profile of the earth flow Neck, see b) for profile position.

5. Results

5.1. Displacement, velocity and structures within the Neck of the Montaguto earth flow

The Neck of the earth flow was actively moving between May and August 2010 (90 days). The average earth-flow velocity over the entire monitoring period ranges from 0.016 m/d (1.4m/90ds) in the upper and lower parts of the kinematic zone, to 0.066 m/d (6m/90ds) in the middle part (fig. 1). Variation of earth-flow velocity along the longitudinal axis of the kinematic zone is shown in the velocity profile in figure 1c. The distribution of displacement and average velocity shown in figure 1b corresponds with three structural sectors characterized by i) normal faults and a linear increase of flow velocity; ii) a peak in velocity where the flow moving core is bounded by strike-slip faults; iii) a decrease of earth-flow velocity associated with the existence of thrust faults and a rapid narrowing of the active flow.

5.2. Displacement and velocity of the Mount Pizzuto earth flow from April 2014 to May 2015

All of the monitoring points moved between April, 2014 and May, 2015 (395 days) and total movement was largely dominated by the horizontal component. Cumulative displacement of moving points ranged from 92 m at monitoring point 20 within the Neck, to 0.4 m at monitoring points 33 and 34 in the Toe. All of the points moved vertically downward. The blue line of figure 4a shows how displacement varies along the length of the flow. Each kinematic zone is characterized by an upslope area of acceleration and a downslope area of deceleration with a peak of displacement in the middle of each zone. An exception to this statement is the earth flow Toe where the displacement vectors linearly decrease toward the toe of the flow. The average daily velocity at the Head of the earth flow ranged from 6 cm/d at point 4 to 17 cm/d at point 2. In the Hopper, the peak of daily velocity is of 4 cm/d at monitoring point 9. Within the Neck, the average daily velocity ranged from 10 cm/d at point 18, to 20 cm/d at point 21. Within the Body, velocity ranged from 17 cm/d at point 24 to 11 cm/d at point 27. At the Toe, the average daily velocity ranged from 1 cm/d at point 28, to 0.1 cm/d at points 33 and 34.

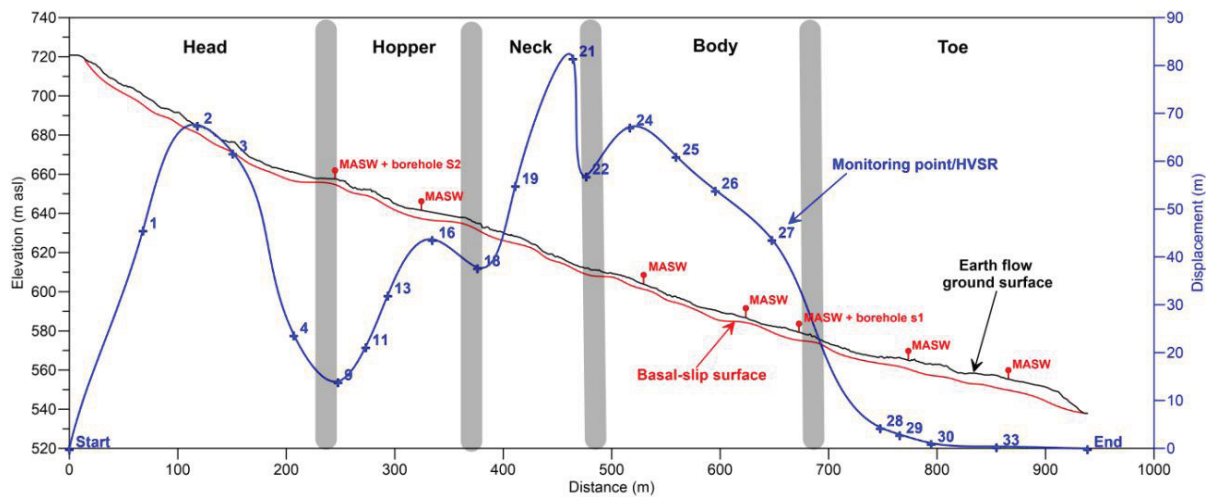


Fig. 4. Longitudinal profile of the Mount Pizzuto earth flow showing the geometry of the basal-slip surface (red line) and the displacement profile (blue line). Start and end points of the displacement profile are arbitrary taken at the beginning and at the end of the topographic profile.

5.3. Displacement, velocity, and structures within the Neck of the Mount Pizzuto earth flow

The average earth flow velocity within the Neck kinematic zone over the April 2014 to May 2015 monitoring period ranged from 0.1 m/d to 0.22 m/d. Variation of earth-flow velocity along the longitudinal axis of the kinematic zone is shown in figure 3b and in the velocity profile of figure 3c. Velocity is characterized by a peak of approximately 90 m/395 days in the middle part of the zone along the right flank of the flow, and decreasing velocity in upper and lower parts of the zone. Where earth-flow material accelerates, normal faults accommodate flow stretching. Decreases in earth-flow velocity (shortening) are accommodated by thrust faults.

6. Discussion

Our results, combined with data from Guerriero et al.¹⁶ and Guerriero et al.¹⁹ indicates that the ground surface of the Montaguto and the Mount Pizzuto earth flows consist of structures indicating different styles of deformation. Guerriero et al.¹⁶ underline that structure distribution can be used to infer the geometry of the basal-slip surface, because of relations between extensional structures and risers in the basal slip surface and compressional structures and trends in the slip surface. These relations form distinct kinematic zones with the Montaguto earth flow. Such structures accommodate deformation caused variation in earth-flow velocity (i.e., acceleration and deceleration). The density of structures appears to be independent of the magnitude of velocity change. For example, the highest

density of extensional structures in the Mount Pizzuto earth flow is in the upper part of the Hopper kinematic zone, whereas the peak acceleration of the flow occurs in the upper part of the Neck (Fig. 4). The high density of normal faults in the Hopper corresponds with the highest value of slope in the basal-slip surface. From this observation, it appears that the slope angle of the basal-slip surface might control the density of deformational structures forming during flow movement.

The displacement profile of the Mount Pizzuto earth flow (Fig. 4) indicates that average velocity (displacement/395 days) varies along the earth flow. Similar variation was also observed within the neck of the Montaguto earth flow. The maximum displacement of the Mount Pizzuto earth flow occurred at point 21 near the neck of the flow. Excluding point 18, displacement increases linearly from the upper end of the Hopper (i.e., point 9) to the earth-flow neck (i.e., point 21). Considering that this part of the flow is characterized by a consistent reduction in the width of the earth-flow, and that field observations indicate constant sediment supply, we infer that displacement in this part of the flow is controlled by both lateral and basal geometry of the basal-slip surface. The presence of a tread causes deceleration of the flow around point 18 while the presence of risers induces acceleration of the flow.

In this context, the velocity profile along kinematic zones appears to have a consistent pattern as demonstrated by Neck zones of the Montaguto and Mount Pizzuto earth flows. These observations suggest that a relation between the velocity profile of an active earth flow and its slip surface geometry does exist and that local variation of flow velocity (i.e. local acceleration and deceleration) are controlled by variations in the slope angle of the slip surface. In other words, the lateral and basal geometry of the basal slip surface controls both the kinematic segmentation of an earth flow and its velocity profile.

7. Conclusion

Our work shows that earth flows are composed of distinct kinematic zones with characteristic longitudinal velocity profiles. Velocity variation along a kinematic zone is consistent with the distribution of structures on the ground surface of the flows. These structures accommodate stretching and shortening of material during movement. Such variation is controlled by the basal and lateral geometry of the slip surface and in particular by local variation of the slope angle. Such geometry seems to also control the density of extensional structures at driving earth-flow elements (i.e., topographic risers).

Acknowledgements

We thank Jeffrey A. Coe and an anonymous reviewer for their constructive reviews of this paper. This research was financed by PRIN 2010-2011 (project 2010E89BPY_001 to F.M. Guadagno).

Reference

1. Baum RL, Messerich J, Fleming RW, 1998. Surface deformation as a guide to kinematics and three-dimensional shape of slow-moving, clay-rich landslides, Honolulu, Hawaii. *Env Eng Geos* 1998;4:283–306.
2. Baum RL, Fleming RW. Use of longitudinal strain in identifying driving and resisting elements of landslides. *Geol Soc Am Bull* 1991;103:1121–1132.
3. Baum RL, Johnson AM. Steady Movement of Landslide Features in Fine-Grained Soils – a Model for Sliding Over an Irregular Slip Surface. Chapter D of Landslide Processes in Utah – Observation and Theory. *US Geol Surv Bull* 1993;1842:D1-D28.
4. Coe JA, Ellis WL, Godt JW, Savage WZ, Savage JE, Michael JA, Kibler JD, Powers PS, Lidke DJ, Debray S. Seasonal movement of the Slumgullion landslide determined from Global Positioning System survey and field instrumentation, July 1998 – March 2002. *Eng Geol* 2003;68:67-101.
5. Coe JA, McKenna JP, Godt JW, Baum RL. Basal-topographic control of stationary ponds on a continuously moving landslide. *Ear Surf/Proc Lan* 2009;34:264 – 279.
6. Diodato N, Guerriero L, Fiorillo F, Esposito L, Revellino P, Grelle G, Guadagno FM. Predicting monthly spring discharge using a simple statistical model. *Wat Res Man* 2014;28:969-978.
7. Fleming RW, Johnson RB, Schuster RL. The reactivation of the Manti landslide. Utah. *US Geol Surv Prof Pap* 1988;1311.
8. Fleming RW, Johnson AM. Structures associated with strike slip faults that bound landslide elements. *Eng Geol* 1989;27:39–114.
9. Fleming RW, Baum RL, Giardino M. Map and description of the active part of the Slumgullion landslide, Hinsdale County, Colorado. *US Geol Surv Misc Inv Ser Map I-2672*, 1999;1:1000-scale. <http://pubs.usgs.gov/imap/i-2672/>
10. Gili JA, Corominas J, Rius J. Using Global Positioning System techniques in landslide monitoring. *Eng Geol* 2000;55:167–192.

11. Giordan D, Allasia P, Manconi A, Baldo M, Santangelo M, Cardinali M, Corazza A, Albanese V, Lollino G, Guzzetti F. Morphological and kinematic evolution of a large earth flow. The Montaguto landslide, southern Italy. *Geom*2013;**187**:61–79.
12. Gomberg J, Bodin P, Savage WZ, Jackson ME. Land- slide faults and tectonic faults, analogs: the Slumgullion earth- flow. Colorado. *Geol*1995;**23**:41–44.
13. Grelle G, Revellino P, Donnarumma A, Guadagno FM. Bedding control on landslides: a methodological approach for computer-aided mapping analysis. *Nat. Hazards Earth Syst. Sci.* 2011;**11**:1395–1409.
14. Guerriero L, Revellino P, Coe JA, Focareta M, Grelle G, Albanese V, Corazza A, Guadagno FM. Multi-temporal maps of the Montaguto earth flow in southern Italy from 1954 to 2010. *J Maps* 2013;**9**:135–145.
15. Guerriero L, Revellino P, Grelle G, Fiorillo F, Guadagno FM. Landslides and Infrastructures: The case of the Montaguto earth flow in Southern Italy. *It J Eng Geol Env*, International Conference Vajont 1963-2013, 2013:447–454.
16. Guerriero L, Coe JA, Revellino P, Grelle G, Pinto F, Guadagno FM. Influence of slip-surface geometry on earth flow deformation, Montaguto earth flow, southern Italy. *Geom* 2014;**219**:285-305.
17. Guerriero L, Revellino P, Mottola A, Grelle G, Sappa G, Guadagno FM. Multi-temporal mapping of the Caforchio earth flow, southern Italy. *Rend On Soc Geol It* 2015;**35**:166 – 169.
18. Guerriero L, Diodato N, Fiorillo F, Revellino P, Grelle G, Guadagno FM. Reconstruction of long-term earth-flow activity using a hydro-climatological model. *Nat Haz*2015;**77**:1-15.
19. Guerriero L, Revellino P, Luongo A, Focareta M, Grelle G, Guadagno FM. The Mount Pizzuto earth flow: deformational pattern and recent thrusting evolution. *J Maps* in review.
20. Hutchinson JN. A coastal mudflow on the Loday clay cliffs at Beltinge, North Kent (England). *Géot*1970;**20**:412–438.
21. Hutchinson JN, Prior DB, Stephens N. Potentially dangerous surges in an Antrim [Ireland] mudslide. *Qu J Eng Geol*1974;**7**:363-376.
22. Keefer DK, Johnson AM. Earthflows: Morphology, mobilization and movement. *US Geol Surv Prof P*1983;**1264**.
23. Nakamura Y. A method for dynamic characteristics estimation of subsurface using microtremor on the ground surface. Railway Technical Research Institute, *Qu Rep*1989;**30**.
24. Nogoshi M, Igarashi T. On the amplitude characteristics of microtremor (part 2). *Zisin = Jishin* 1971;**24**:26–40.
25. Pescatore T, Di Nocera S, Matano F, Pinto F. L'unità del Fortore nel quadro della geologia del settore orientale dei Monti del Sannio (Appennino meridionale). *Boll Soc Geol Ital* 2000;**119**:587-601.
26. Pinto F, Guerriero L, Revellino P, Grelle G, Senatore MR, Guadagno FM. Structural and lithostratigraphic control of earth-flow evolution, Montaguto earth flow, southern Italy. *J Geol Soc Lon* in review.
27. Revellino P, Grelle G, Donnarumma A, Guadagno F.M. Structurally-controlled earth flows of the Benevento Province (Southern Italy). *Bull. Eng. Geol. Env.* 201;**69**:487-500.